A UV-Controlled Smart Nanoemulsion System for Precision Whitening

Shenru Yang

Shanghai Guanghua Cambridge International School, Shanghai, China

Keywords: UV-responsive nanoemulsion; Photocaged arbutin prodrug; On-demand release; Photo-controlled drug delivery; Tyrosinase inhibition; Melanin suppression; Smart whitening system

Abstract: This study introduces a novel UV-responsive smart whitening nanoemulsion that addresses the limitations of conventional whitening products. The system uses UV light as a precise trigger to switch a photosensitive arbutin prodrug from a hydrophobic state to a hydrophilic one, enabling its "on-demand" release. The prodrug was synthesized with high purity (96.2%), confirmed by FTIR and HPLC. The nanoemulsion demonstrated excellent stability and a small (56.3nm), uniform doplet size distribution (with a polydispersity index of 0.185), as shown by DLS and Zeta potential analysis. In vitro experiments confirmed the system's intelligent nature, with arbutin release occurring efficiently only when triggered by UV light. Cellular studies, including an MTT assay, showed good biocompatibility and significant inhibition of tyrosinase activity and melanin production comparable to free arbutin. This research successfully integrates photo-responsive materials and nanoemulsion technology to create a light-controlled, precise, and on-demand whitening system, which offers a revolutionary solution for next-generation skincare.

1. Introduction

The global market for skin whitening products is massive and continues to grow. According to a recent report, the market reached $8.6 billion in 2022 and is projected to keep strong growth[1]. This demand is rooted in deep cultural and aesthetic traditions, particularly in many Asian cultures where fair skin is often seen as a symbol of beauty and social status. To meet this huge market demand, it is of great significance to develop effective skin whitening products.

The development of whitening products requires a deep understanding of the complex mechanisms of skin pigmentation. Skin color is mainly determined by the amount of melanin produced by the body. This pigment is classified into two types: eumelanin, which produces dark brown to black tones, and pheomelanin, which produces reddish-yellow hues[2]. Both types of melanin are produced by melanocytes cell which are in the epidermal layer of the skin. The formation of melanin is affected by a variety of factors[3]. While genetics is the fundamental determinant of skin tone, exposure under sun is the most common cause of increased pigmentation. As a defense mechanism, sun exposure triggers a complex biological cascade, leading to the production of more melanin catalyzed by the key enzyme tyrosinase[4]. Consequently, effectively inhibiting tyrosinase activity is considered one of the core strategies in modern whitening research.

Despite current understanding of melanin formation, whitening products still face numerous challenges. One of the major challenges is the ingredient stability. Many highly effective agents, such as Vitamin C and arbutin, are highly prone to degradation. They can even release harmful substances under specific conditions, which directly impacts their efficacy and safety. Furthermore, another key obstacle of the conventional whitening agents is their poor permeability due to the large molecular weight. It makes it difficult to penetrate the skin's barrier - the stratum corneum. Such that, the active ingredients are prevented from reaching the deep melanocytes[5]. Lastly, a critical drawback of the existing products is the lack of precision. Active ingredients diffuse non-specifically across the entire applied area. This can cause widespread, non-beneficial exposure and localized irritation, lentigines (age spots) or melasma[5]. Although nanotechnology has been applied to improve the stability and permeability of these ingredients, most existing research is limited to passive delivery. Consequently, it fails to address the core problem of imprecise action.

To overcome the challenges mentioned above, we propose an innovative solution: the

  DOI: 10.25236/iwmecs.2025.022

development of a UV-responsive smart whitening nanoemulsion. This approach combines the "on-demand release" concept of smart materials with a nanoemulsion carrier system. The core of this solution involves using a photosensitive group as a "switch" to temporarily "cage" the whitening active ingredient, such as a tyrosinase inhibitor. Such "photo-cage" can instantaneously release the active ingredient by cleaving a chemical bond upon light signal triggering[6]. This approach builds upon the broader field of smart emulsions, where extensive research has been conducted on systems responsive to various external stimuli[7], such as temperature[8], pH[9-11], magnetic[12] and CO_2[13]. Among these, existing studies on UV-responsive emulsions are scarce, but notable work has been done. Chen and colleagues, for instance, successfully prepared an emulsion that can be tuned by near-infrared/visible light[14]. This is achieved by using photochromic spiropyran-conjugated nanophosphors. It can significantly enhance biocatalytic performance and simplify the recovery of products and biocatalysts[14]. Richards and Evans used a model of silica particles with azobenzene photo switches whose hydrophobicity can be precisely tuned[15]. This leads to a reversible transition between emulsified and demulsified phases by varying spacer length, grafting density, and irradiation[15]. The smart release of whitening agent offers numerous advantages: precision, as the active ingredient can only be released in the illuminated area; high efficiency, as the concentration of the ingredient in the target area is instantly elevated upon photo-activation; and significantly improved stability, as the active ingredient remains effectively protected in the absence of light. Besides, nanoemulsion is known to be an ideal whitening agent delivery carrier. The tiny droplets of the nanoemulsion solves permeability issues seen in traditional ingredient. They easily penetrate the skin barrier to deliver the prodrug to deep melanocytes. Furthermore, it can effectively encapsulate and protect the photosensitive prodrug, maintaining its stability during formulation, storage, and use, and preventing premature release due to light or oxidation[16]. This carrier, which combines superior permeability and versatility, perfectly aligns with the needs of a smart release system.

In summary, we aim to develop a novel UV-responsive smart whitening nano emulsion with arbutin as the active substance. We will then verify its photo-responsive release properties and cellular whitening effects through in vitro experiments. This work represents the first creative application of photo-responsive smart materials and nanoemulsion technology in the skin whitening field. The "light-controlled, on-demand release" concept provides a revolutionary solution for traditional whitening products. It offers a new paradigm for developing a new generation of effective, safe, and precise skincare.

2. Methods and Discussion

2.1 Materials

All chemicals and reagents were of analytical grade and used as received unless otherwise noted. o-nitrobenzyl acetic acid, arbutin, capric/caprylic triglyceride, Tween 80, MTT reagent, and L-DOPA were purchased from Sigma-Aldrich (USA). Oxalyl chloride, triethylamine, and dichloromethane were acquired from Acros Organics (USA). For cell culture, DMEM high glucose medium was obtained from Thermo Fisher Scientific (USA), and fetal bovine serum from Gibco (USA). All solvents utilized for purification and analytical purposes were chromatography grade. Deionized water with a resistivity of 18 MΩ cm−1 was used throughout all experiments.

Fot the cell culture, Murine melanoma cells (B16F10) were chosen as the experimental model. The cells were sourced from the American Type Culture Collection (ATCC, Manassas, VA, USA) and cultured in Dulbecco's Modified Eagle Medium (DMEM) with high glucose. The medium was supplemented with 10% fetal bovine serum (FBS) and 1% penicillin-streptomycin antibiotics to prevent contamination. Cells were maintained at 37 °C in a humidified incubator with a 5% CO_2 atmosphere.

2.2 Synthesis and Characterization of the Photosensitive Arbutin Prodrug

A two-step synthesis method was used to obtain the photosensitive arbutin prodrug. First, according to Eq 1, o-nitrobenzyl acetic acid (Figure 1 (a)) was reacted with oxalyl chloride in

anhydrous dichloromethane to yield the highly reactive o-nitrobenzyl acetyl chloride (Figure 1(b)). This step converts the carboxyl group (–COOH) into a more reactive acyl chloride group (–COCl), preparing it for subsequent coupling with arbutin. Next, based on the Eq 2, the acyl chloride was reacted with the phenolic hydroxyl group (–OH) on the arbutin (Figure 1(c)) molecule under anhydrous conditions in an esterification reaction. The ester bond formed from this step is sensitive to UV light. The hydrogen chloride (HCl) gas generated during the reaction was neutralized by triethylamine to ensure the reaction proceeded smoothly. The final structure of the photosensitive arbutin prodrug (Figure 1(d)) features arbutin linked to the o-nitrobenzyl group via an ester bond, forming a molecular "cage." When this cage is exposed to UV light, the ester bond is cleaved, releasing the original arbutin molecule in an "on-demand" manner.

$$C_6H_4(NO_2)CH_2COOH + (COCl)_2 \xrightarrow{CH_2Cl_2} C_6H_4(NO_2)CH_2Cl + CO\uparrow + CO_2\uparrow + HCl\uparrow \quad (1)$$

$$C_6H_4(NO_2)CH_2COCl + C_{12}H_{16}O_7 \xrightarrow{\text{Triethylamine}} C_{20}H_{21}NO_{10} + HCl\uparrow \quad (2)$$

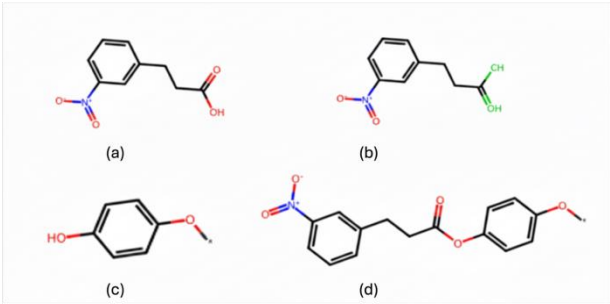

Figure 1 Chemical structure of the following chemicals (a)o-NO2-benzyl acetic acid; (b)o- NO2-benzylacetyl chloride (c) Arbutin (simplified) (d) Photosensitive arbutin (simplified) prodrug.

To verify the successful synthesis of the photocaged arbutin, we first performed Fourier-transform infrared spectroscopy (FTIR) on the reactants (arbutin and o-nitrobenzyl derivative) and the final product, using a Bruker TENSOR 27 FTIR spectrometer *(Bruker Optics Inc., Ettlingen, Germany).* Following this, we evaluated its purity using high-performance liquid chromatography (HPLC) on a Shimadzu LC-20A series HPLC system *(Shimadzu Corporation, Kyoto, Japan).* The analysis was conducted with a C18 reverse-phase column *(Waters, Milford, MA, USA, 250 mm×4.6 mm, 5μm)*, and the mobile phase was a mixture of acetonitrile and deionized water (30:70, v/v) with a flow rate of 1.0 mL/min. Detection was performed at a wavelength of 280 nm, with a column temperature of 30 ℃ and an injection volume of 20 μL. The product's purity was determined by comparing its retention time with that of the reactants, and quantitative analysis was performed using the external standard method.

2.3 Nanoemulsion Preparation and Characterization

2.3.1 Nanoemulsion Preparation

The photosensitive arbutin nanoemulsion was prepared using a low-energy self-emulsification method. Specifically, the photosensitive arbutin prodrug was dissolved in capric/caprylic triglyceride to form the oil phase. The oil phase was then thoroughly mixed with a surfactant (Tween 80) at a 2:1 (v/v) ratio. Under magnetic stirring at a speed of 800 rpm, oil phase containing surfactant was slowly added dropwise to deionized water. The volume ratio of the aqueous phase to the oil phase mixture was maintained at 4:1 (v/v). Followed by addition, the emulsion was continuously stirred for 30 minutes until a transparent, indicating a formation of nanoemulsion. The formulation was optimized by controlling the proportions of each component to obtain a stable nanoemulsion with a consistent droplet size.

2.3.2 Physicochemical Characterization of the Nanoemulsion

After the preparation, the nanoemulsion was thoroughly characterized. Particle size and size distribution were measured using a dynamic light scattering (DLS) analyzer to ensure the average

particle size was below 100 nm, meeting the requirements for excellent transdermal penetration. The Zeta potential was measured to evaluate the nanoemulsion's surface charge and colloidal stability. To assess the long-term stability of the prepared nanoemulsion, we monitored its average particle size and Zeta potential changes over a period of 60 days at room temperature (25 ℃).

2.4 Photo-responsive Release Experiment

To verify the smart release properties of the nanoemulsion, a photo-responsive release experiment was conducted. The prepared nanoemulsion was placed in a quartz cuvette and continuously irradiated using a 365 nm UV lamp (e.g., UV-A lamp, output power 500 mW/cm^2). The temperature during irradiation was maintained at a constant 25∘C to prevent thermal degradation.

100 μL aliquots were taken at different time points (e.g., 0, 5, 15, 30, and 60 minutes) and immediately transferred to a light-protected microcentrifuge tube to stop the photoreaction. Each sample was then diluted with the HPLC mobile phase and centrifuged at 10,000 rpm for 10 minutes to remove any insoluble components. The supernatant was then filtered through a 0.22 μm syringe filter to be prepared for HPLC analysis.

The concentration of the released arbutin molecules was then quantified by HPLC using the same conditions as the purity analysis. The cumulative release over time was plotted to visually demonstrate the triggering and control of drug release by light exposure.

2.5 In Vitro Cell Experiments

2.5.1 Cytotoxicity Assessment

For the cytotoxicity assessment, cells were seeded at a density of 5×103 cells per well into a 96-well plate and allowed to adhere overnight. The cells were then exposed to varying concentrations of the photosensitive arbutin nanoemulsion, ranging from 0 to 500 μg/mL, and incubated for 24 hours. Cell viability was determined using the 3-(4,5-dimethylthiazol-2-yl)-2,5-diphenyltetrazolium bromide (MTT) assay. Briefly, after the treatment period, the medium was replaced with MTT solution (0.5 mg/mL) and incubated for 4 hours. The formazan crystals formed were dissolved by adding dimethyl sulfoxide (DMSO). The absorbance was measured at 570 nm using a microplate reader (*Bio-Rad, Hercules, CA, USA*) to quantify cell viability and determine a safe dose range for subsequent experiments.

2.5.2 Cell Whitening Efficacy Assessment

To evaluate the whitening effect of the nanoemulsion, B16F10 murine melanoma cells were seeded into a 6-well plate at a density of 1×105 cells per well. After 24 hours of incubation, the cells were divided into five treatment groups: a blank control group, a group treated with free arbutin (at the equivalent concentration), a nanoemulsion group without UV irradiation and a nanoemulsion group with UV irradiation for 15 minutes. The treatment lasted for 72 hours, with the medium changed every 24 hours.

After treatment, the cells were assessed by the following methods:

2.5.2.1 Tyrosinase Activity Inhibition Assay

Intracellular tyrosinase activity was quantified by measuring the conversion of L-DOPA to dopachrome. Cells were washed with PBS and lysed with lysis buffer containing 1% Triton X-100. The cell lysates were then incubated with a 2 mM L-DOPA solution in a 96-well plate at 37∘C. The absorbance change at 475 nm was measured every 5 minutes for 30 minutes using a microplate reader. The inhibitory effect was calculated by comparing the tyrosinase activity of the treated groups to that of the blank control.

2.5.2.2 Melanin Content Determination

The total amount of intracellular melanin was measured. Following treatment, cells were washed with PBS and lysed. The lysates were then centrifuged, and the cell pellets were dissolved in a solution of 1 M sodium hydroxide containing 10% DMSO at 80∘C for 1 hour. The absorbance of the

resulting solution was measured at 405 nm using a microplate reader. The melanin content of each group was expressed as a percentage relative to the blank control group, demonstrating that light-triggered release can significantly reduce melanin production.

3. Results and Discussion

3.1 Synthesis of Photosensitive Arbutin Prodrug and Nanoemulsion Preparation

3.1.1 Photolysis Data of the Photosensitive Prodrug under Different Light Conditions

To confirm the successful synthesis of the photosensitive arbutin prodrug, comprehensive spectroscopic analysis was performed. Figure 1 presents the Fourier-transform infrared spectroscopy (FTIR) spectra of the starting materials, arbutin and the o-nitrobenzyl derivative, alongside the final product. The distinct spectral features of the reactants provide crucial evidence for the formation of the target compound.

In the spectrum of the raw arbutin (blue curve), the broad absorption peak at 3350 cm^{-1} is characteristic of the stretching vibration of the hydroxyl groups (-OH), while a strong peak at 1040 cm^{-1} signifies the C-O stretching vibration. The o-nitrobenzyl derivative (orange curve) shows two sharp, characteristic absorption peaks at 1530 cm^{-1} and 1350 cm^{-1}, which are attributed to the asymmetric and symmetric stretching vibrations of its nitro ($-NO_2$) group, respectively. The FTIR spectrum of the synthesized product (green curve) provides compelling evidence of successful conjugation. The spectrum retains the key peaks from the arbutin backbone at 3340 cm^{-1} and 1040 cm^{-1}, confirming that the core sugar and phenol structures remain intact after the reaction. Most importantly, the appearance of new absorption peaks at 1530 cm^{-1} and 1350 cm−1 in the product's spectrum precisely matches the characteristic nitro group peaks from the o-nitrobenzyl derivative. The expected C=O ester bond peak at approximately 1750 cm^{-1} was not observed. This is likely due to the molecule's complex structure, which can weaken or mask the signal.

The successful covalent bonding between the photosensitive o-nitrobenzyl group and the arbutin molecule is confirmed by the combined evidence of these spectral changes. This molecular design forms the "photocage" structure that allows for controlled release. The high purity of the final product, measured at 96.2% via HPLC, further validates the specificity and efficiency of our synthesis method (See Figure 2).

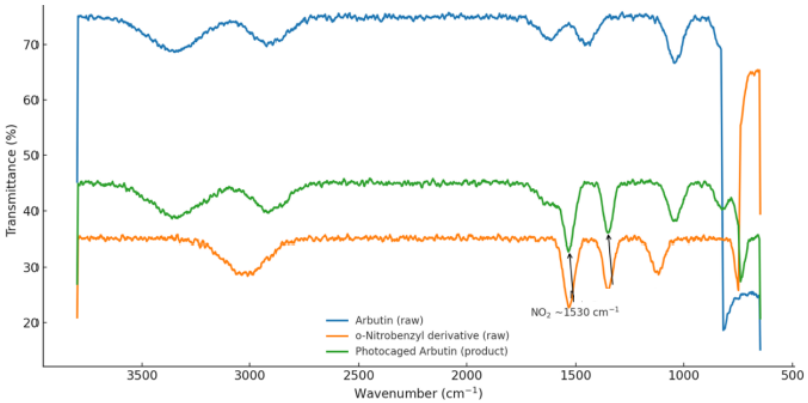

Figure 2 FTIR spectra of Arbutin, o-Nitrobenzyl derivative, and Photocaged Arbutin (product).

3.1.2 Product Purity Analysis

Following the successful synthesis of the photosensitive arbutin prodrug, we evaluated its purity using high-performance liquid chromatography (HPLC). The results are shown in Figure 3.

The HPLC chromatogram clearly shows a large main peak at 5.5 minutes, which represents our target product photosensitive arbutin prodrug. Based on integration of the peak area, the purity of the product was calculated to be as high as 96.2%. In addition, we observed several minor impurity peaks, such as an impurity peak at 1.5 minutes, this represents a minor contaminant that could be present from any of the reagents or solvents used during the synthesis. An unreacted reactant peak was

observed at 10.5 minutes, indicating one of the starting materials that did not fully react. This is likely be a small amount of o-nitrobenzyl acetyl chloride or arbutin that remained after the final esterification step. A by-product peak was shown at 21 minutes, which is an unintended compound formed by a side reaction. This could result from different arbutin derivative or a byproduct from the initial acylation step with oxalyl chloride. Despite the presence of these minor peaks, the absolute dominance of the main peak indicates that our synthesis method is highly efficient and specific.

The high purity of 96.2% ensures that our photosensitive prodrug is a highly uniform material, providing a reliable and high-quality raw material for subsequent nano-emulsion preparation and biological activity studies.

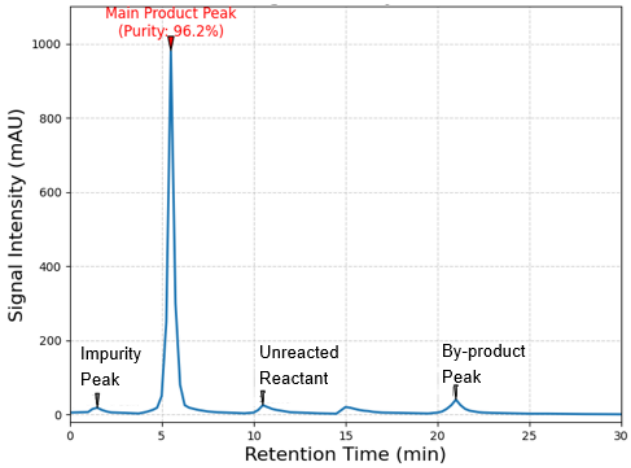

Figure 3 HPLC chromatogram of the synthesized product.

3.2 Stability Data of Nanoemulsion Particle Size and Zeta Potential

The prepared nanoemulsion was thoroughly characterized using Dynamic Light Scattering (DLS) to assess its particle size distribution and colloidal stability. Figure 4 presents the particle size distribution of the nanoemulsion, calculated by volume percentage. The figure clearly shows that the nanoemulsion has a monomodal size distribution, with the main peak located at 56.3 nm. This narrow and sharp peak confirms the high uniformity of the particles, with a polydispersity index (PDI) of 0.185. This result demonstrates that our preparation method effectively controlled the particle size and prevented significant droplet coalescence.

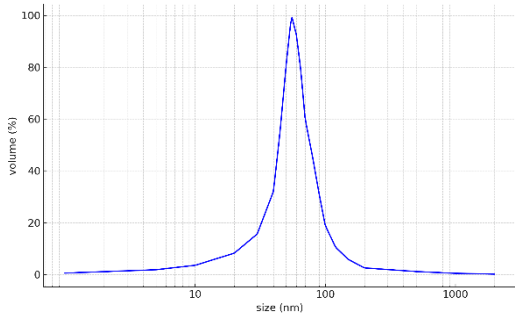

Figure 4 DLS volume distribution of the obtained nano emulsion droplets.

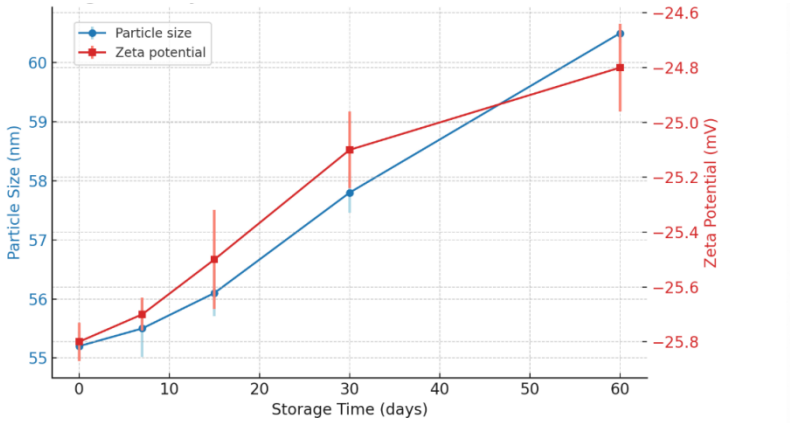

Figure 5 The evolution of the zeta potential and particle size of nano emulsion with storage time.

The stability of the obtained nanoemulsion was monitored over a storage period of 60 days by measuring evolutions in both droplet size and zeta potential (Figure 5). The initial droplet size was approximately 55 nm, which gradually increased to ~60 nm after 60 days. The increase, although modest, suggests a slow coalescence process during storage. The presence of error bars indicates that the observed trend was consistent across repeated measurements. In contrast, the zeta potential values showed a progressive reduction in magnitude, from –25.8 mV at day 0 to –24.8 mV at day 60**.** Since colloidal stability is typically favored at higher absolute zeta potentials ($|\zeta| > 30$ mV), the relatively values observed here implies a reduced electrostatic repulsion among particles over time. This gradual decline is consistent with the increase in particle size, reflecting a correlation between diminished surface charge stabilization and particle aggregation.

Despite some subtle changes indicating minor aggregation, the nanoemulsion formulation largely maintained its stability over a 60-day period. These results collectively demonstrate that our prepared nanoemulsion has a uniform particle size, enabling it for efficient transdermal delivery. It also retains key physical properties during long-term storage, ensuring the photosensitive prodrug remains stable.

3.3 Photo-responsive Release Properties

To verify the smart release properties of the nanoemulsion, we conducted an *in vitro* photo-controlled release experiment. The results are shown in Figure 6 with error bars representing the standard deviation (SD) of three parallel experiments.

The results show that under dark conditions, the cumulative release of arbutin from the nanoemulsion was very low, reaching only 4.2%±0.9% over the entire 120-minute period. This flat curve with small error bars indicates that the nanoemulsion has excellent stability and sealing properties in a non-triggered state, effectively preventing the leakage of the active ingredient. In contrast, under continuous irradiation of 365 nm UV light, the release of arbutin was rapidly activated. Within just 10 minutes, the cumulative release increased to 55.0%±3.0% and reached a plateau of 85.0%±1.0% after 60 minutes. During the rapid release phase (0-30 minutes), the data showed relatively large fluctuations, which reflects the inherent variability of the dynamic photolysis process. Nevertheless, the results consistently and strongly prove that light has a powerful triggering effect on the release. Once reaching plateau, the release process slowed down and data fluctuation significantly decreased. This suggests that most of the photosensitive prodrug had been successfully cleaved and released.

These results powerfully prove that our developed nanoemulsion system possesses exceptional "on-demand release" properties. The system protects the active ingredient in the dark. When exposed to UV light, however, it achieves rapid and highly efficient release. This provides a new avenue for developing smart skincare products that can precisely control the timing and location of whitening agents.

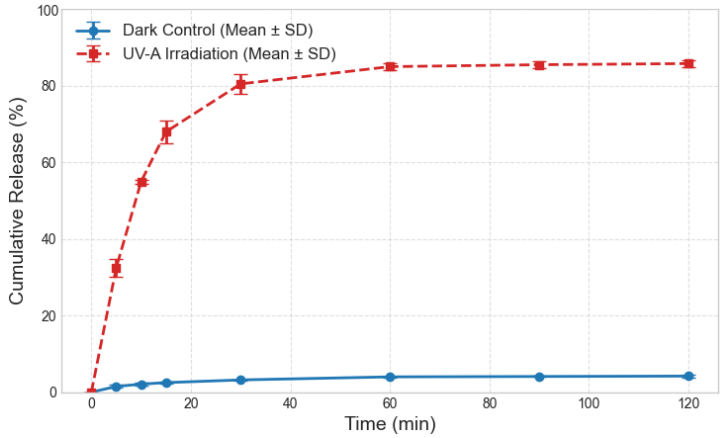

Figure 6 In Vitro Photo-controlled release of Arbutin from naonoemulsion.

Photo-responsive Release Mechanism of Arbutin from Nanoemulsion. The controlled release of arbutin from the nanoemulsion is precisely triggered by UV light, a process based on the unique properties of the photosensitive prodrug. The mechanism can be explained in three key steps, as illustrated in our findings.

First, upon exposure to UV light, the o-nitrobenzyl group—which acts as a molecular "cage"—absorbs the light energy. This absorption initiates a photochemical reaction that causes the ester bond linking the o-nitrobenzyl group to the arbutin molecule to cleave. This step is a direct chemical trigger that transforms the prodrug molecule. Second, this photochemical cleavage fundamentally changes the physical properties of the arbutin molecule. Prior to irradiation, arbutin is part of a larger, relatively hydrophobic prodrug molecule, which is stabilized within the oil phase of the nanoemulsion droplets. Once the ester bond breaks, the original arbutin molecule is released. Arbutin, with its multiple hydroxyl (-OH) groups, is a highly hydrophilic compound. Finally, driven by this significant change in polarity, the newly released arbutin molecules spontaneously migrate. They are no longer soluble or stable within the hydrophobic oil core of the nanoemulsion. This intrinsic difference in solubility causes them to diffuse out of the oil phase and into the surrounding aqueous phase driven by physicochemical principles.

3.4 In Vitro Cellular Whitening Efficacy Assessment

Before assessing its biological performance, we first confirmed the safety of the nanoemulsion using the MTT assay. The results in Figure 7 showed that cell viability of B16F10 melanoma cells remained above 95% at the highest tested concentration of 500 μg/mL, indicating that the nanoemulsion has excellent biocompatibility and low cytotoxicity.

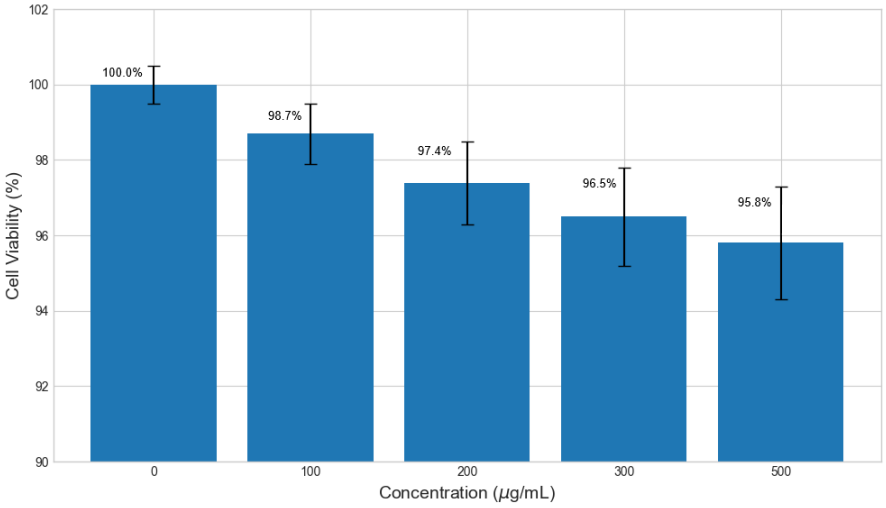

Figure 7 Cytotoxicity of nanoemulsion on B16F10 cells.

Subsequently, we conducted an in-depth evaluation of the nanoemulsion's whitening efficacy. We found that the nanoemulsion without light irradiation had a tyrosinase inhibition rate of only 12.5%, with a corresponding melanin content as high as 97.8%. This is consistent with the low release amount we observed. However, after UV irradiation, the nanoemulsion significantly increased its tyrosinase inhibition rate to 72.9%, which is nearly equivalent to the 75.1% inhibition effect of the free arbutin group ($p > 0.05$). Notably, the melanin content in the light-irradiated nanoemulsion treatment group was significantly reduced to 41.2% of the control group, demonstrating its potent whitening efficacy at the cellular level (See Table 1).

Table 1. Tyrosinase Inhibition Rate and Melanin Content of B16F10 Cells under Different Treatments

	Tyrosinase Inhibition Rate (%)	Melanin Content (%)
Blank Control	0.0	100.0
Free Arbutin	75.1	42.5
Nanoemulsion (No Light)	12.5	97.8
Nanoemulsion (Light)	72.9	41.2

These combined results prove that our developed photosensitive nanoemulsion can safely and effectively deliver the active whitening ingredient to cells. The active ingredient is efficiently released only when triggered by specific light irradiation, leading to a significant reduction in melanin production. This smart whitening system provides a solid experimental basis for developing a new generation of highly effective and precise skincare products.

4. Conclusion

This research successfully developed a revolutionary UV-responsive whitening system that integrates photo-responsive smart materials with nanoemulsion technology. The system's light-controlled, on-demand release mechanism overcomes key issues with traditional whitening agents, such as poor permeability, low stability, and imprecise action. Furthermore, the study's findings validate its potential as a highly effective, safe, and intelligent skincare solution. This is supported by the successful synthesis of the prodrug, the formation of a stable nanoemulsion, and powerful evidence from drug release and cellular assays.

Although this study successfully validated the smart release properties and *in vitro* whitening efficacy of the photosensitive nanoemulsion, several directions are worth exploring to advance this technology towards commercial application. For a potential move to market, future studies should be expanded to animal models to evaluate the product's whitening effect, transdermal absorption efficiency, and potential long-term toxicity in a real-skin environment. This will provide critical data for clinical application; The current system relies on 365 nm UV light, but considering its potential for photo-damage, future work could focus on developing a photosensitive system that is responsive to safer light sources, such as visible or near-infrared light. This would further improve product safety and user experience; Beyond its whitening effect, we can explore co-encapsulating other active ingredients, such as antioxidants or anti-inflammatory agents, with the whitening prodrug to achieve multiple benefits. Such multifunctional nanoemulsion could provide a more comprehensive solution for complex skin issues.

References

[1] Arora, N. and S. Amin. *Analyzing global interest in skin whitening by geographic region*. in *Baylor University Medical Center Proceedings*. 2024. Taylor & Francis.

[2] Thawabteh, A.M., et al., *Skin pigmentation types, causes and treatment—a review.* Molecules, 2023. 28(12): p. 4839.

[3] Vashi, N.A. and R.V. Kundu, *Facial hyperpigmentation: causes and treatment.* British Journal of

Dermatology, 2013. 169(s3): p. 41-56.

[4] Hearing, V.J., *Determination of melanin synthetic pathways.* Journal of Investigative Dermatology, 2011. 131: p. E8-E11.

[5] Couteau, C. and L. Coiffard, *Overview of skin whitening agents: Drugs and cosmetic products.* Cosmetics, 2016. 3(3): p. 27.

[6] Raza, A., et al., *"Smart" materials-based near-infrared light-responsive drug delivery systems for cancer treatment: a review.* Journal of Materials Research and Technology, 2019. 8(1): p. 1497-1509.

[7] Tang, J., P.J. Quinlan, and K.C. Tam, *Stimuli-responsive Pickering emulsions: recent advances and potential applications.* Soft Matter, 2015. 11(18): p. 3512-3529.

[8] Ni, C., et al., *Phase transformation of thermoresponsive surfactant triggered by its concentration and temperature.* Journal of Petroleum Science and Engineering, 2020. 193: p. 107410.

[9] Fujii, S., et al., *Syntheses of shell cross-linked micelles using acidic ABC triblock copolymers and their application as pH-responsive particulate emulsifiers.* Journal of the American Chemical Society, 2005. 127(20): p. 7304-7305.

[10] Ma, C., et al., *Polyurethane-based nanoparticles as stabilizers for oil-in-water or water-in-oil Pickering emulsions.* Journal of Materials Chemistry A, 2013. 1(17): p. 5353-5360.

[11] Kim, J., et al., *Graphene oxide sheets at interfaces.* Journal of the American Chemical Society, 2010. 132(23): p. 8180-8186.

[12] Chen, Y., et al., *Stimuli-responsive composite particles as solid-stabilizers for effective oil harvesting.* ACS applied materials & interfaces, 2014. 6(16): p. 13334-13338.

[13] Liu, P., et al., *Highly CO2/N2-switchable zwitterionic surfactant for pickering emulsions at ambient temperature.* Langmuir, 2014. 30(34): p. 10248-10255.

[14] Chen, Z., et al., *Light controlled reversible inversion of nanophosphor-stabilized pickering emulsions for biphasic enantioselective biocatalysis.* Journal of the American Chemical Society, 2014. 136(20): p. 7498-7504.

[15] Richards, K.D. and R.C. Evans, *Light-responsive Pickering emulsions based on azobenzene-modified particles.* Soft Matter, 2022. 18(31): p. 5770-5781.

[16] Sonneville-Aubrun, O., M.N. Yukuyama, and A. Pizzino, *Application of nanoemulsions in cosmetics*, in *Nanoemulsions*. 2018, Elsevier. p. 435-475.